JACC Vol. 23, No. 2
February 1994:514–24

Nonlinearity of the Left Ventricular End-Systolic Wall Stress–Velocity of Fiber Shortening Relation in Young Pigs: A Potential Pitfall in Its Use as a Single-Beat Index of Contractility

ANIRBAN BANERJEE, MD,* MICHAEL MORRIS BROOK, MD,
ROBERT JOHANNES MENNO KLAUTZ, MD, DAVID FRANK TEITEL, MD
San Francisco, California

Objectives. **We sought to evaluate in the young heart the primary assumptions on which the current use of the mean "velocity of fiber shortening corrected for heart rate" as a noninvasive index of contractility are based.**

Background. **End-systolic wall stress–velocity of fiber shortening relation has been applied as a single-beat, load-independent index of contractility in children. This use is based on poorly validated assumptions of linearity, parallel shifts with changing contractile state and inotropic sensitivity of the end-systolic wall stress–velocity of fiber shortening relation.**

Methods. **In eight anesthetized young piglets, 5F micromanometric catheters were placed in the ascending aorta and balloon occlusion catheters in the descending aorta. End-systolic wall stress and velocity of fiber shortening were calculated from aortic pressure and M-mode echocardiography under six conditions: in three contractile states 1) baseline, 2) increased contractility during dobutamine infusion (10 μg/kg per min), and 3) decreased contractility after propranolol injection (1 mg/kg), each at two afterload states (normal and increased load by partial aortic occlusion).**

Results. **Dobutamine increased and propranolol decreased afterload-matched velocity of fiber shortening corrected for heart rate significantly to 140% and 77% of baseline, respectively. However, the slope of end-systolic wall stress–velocity of fiber shortening relation was much greater (251% of baseline) during dobutamine infusion, which also significantly decreased wall stress, and was much less (27% of baseline) after propranolol injection, which increased wall stress.**

Conclusions. **The velocity of fiber shortening corrected for heart rate did change predictably with changes in contractility and as such can be used noninvasively in the temporal evaluation of individual patients undergoing therapeutic interventions or to define the natural history of a disease process. However, the relation on which it is based is not defined by parallel straight lines across contractile states, so that abnormal single point measurements may reflect only the nonlinearity of the relation rather than abnormalities in contractility. Thus, we recommend that the end-systolic wall stress–velocity of fiber shortening relation should not be used as a single-beat index of contractility.**

(J Am Coll Cardiol 1994;23:514–24)

Although the quest for a sensitive and specific index of myocardial contractility that is insensitive to changes in heart rate and loading conditions has been ongoing for several decades, such an index remains elusive. Contractility has been evaluated in a variety of planes on the basis of different intrinsic properties of muscle. Based on the length-tension relation, indexes in the pressure-volume plane have been described, including the end-systolic pressure-volume relation (1) and the preload-recruitable stroke work index (2). Based on the force-frequency relation, postextrasystolic potentiation has been explored by a variety of methods (3–5). Additionally, based on the force-velocity relation, the velocity of fiber shortening has been analyzed at normal load (6,7) and, by extrapolation, at zero (8,9) load. This force-velocity relation is a basic property of skeletal muscle (10,11) and is presumed to be one of cardiac muscle, describing a hyperbolic relation between the force against which a muscle contracts and the velocity at which it shortens (Fig. 1A).

Recently, Colan et al. (12) developed an adaptation of this relation using echocardiographic techniques. They generated a single normal relation between mean velocity of fiber shortening corrected for heart rate and end-systolic wall stress across a wide range of afterload and ages. To evaluate contractility, this mean velocity of fiber shortening corrected for heart rate at a known end-systolic wall stress is plotted on this relation; a value above the linear relation represents an increased contractile state, whereas a value below repre-

From the Cardiovascular Research Institute and the Department of Pediatrics, University of California, San Francisco, San Francisco, California. This project was supported by an Academic Senate Opportunity Award and a Research Evaluation and Allocation Committee Harris Award of the University of California, San Francisco. Drs. Banerjee and Brook were supported by Training Grant HL07544 from the National Institutes of Health, Bethesda, Maryland.

Manuscript received January 20, 1993; revised manuscript received August 23, 1993, accepted September 8, 1993.

All editorial decisions for this article, including selection of referees, were made by a Guest Editor. This policy applies to all articles with authors from the University of California, San Francisco.

*Present address: Dr. Anirban Banerjee, Division of Cardiology, Children's Hospital Medical Center, Cincinnati, Ohio 45229.

Address for correspondence: Dr. David Frank Teitel, Box 0130, University of California, San Francisco, San Francisco, California 94143.

0735-1097/94/$7.00

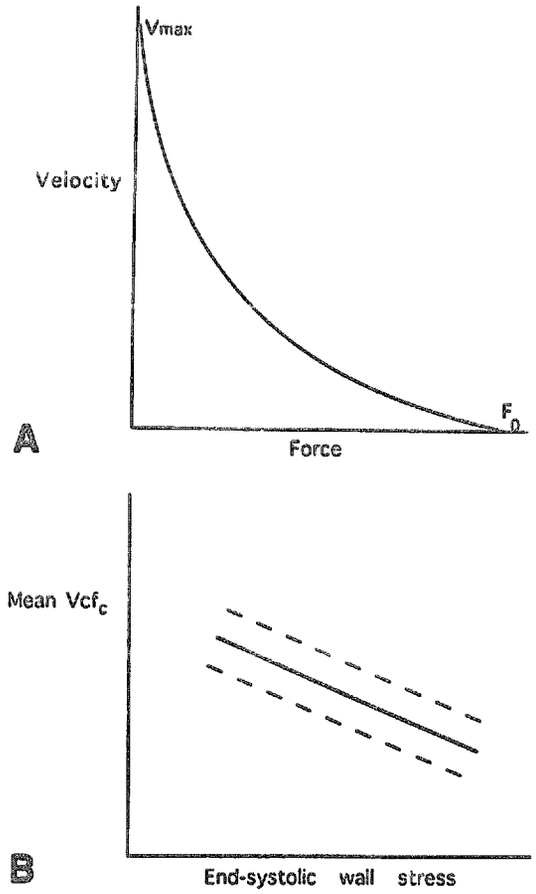

Figure 1. Force-velocity and end-systolic wall stress–velocity of fiber shortening relations. **A**, The force-velocity relation approximates a rectangular hyperbola, reaching maximal velocity (Vmax) when a contraction is fully unloaded and maximal force (F_0) when a contraction is isometric. **B**, Idealized representation of the end-systolic wall stress–velocity of fiber shortening relation as previously described (12), showing a linear relation across wall stress independent of age and geometry. Vcf_c = mean velocity of fiber shortening corrected for heart rate.

sents a decreased contractile state (Fig. 1B). This index subsequently has been used to assess myocardial contractility in a variety of clinical situations, including after arterial switch operations (13), in patients with end-stage renal disease undergoing dialysis and renal transplantation (14), in patients after the Fontan operation (15) and in pediatric patients with human immunodeficiency virus (HIV) infection (16).

However, the use of velocity of fiber shortening corrected for heart rate as a single-beat index of contractility is based on several assumptions. First, it requires that the end-systolic wall stress–velocity of fiber shortening relation is linear and that changes in contractile state are associated with parallel shifts in the relation. Second, it requires that the relation is sensitive to changes in contractile state but insensitive to changes in heart rate. Third, it requires that hearts of different sizes, mass/volume ratios and shapes generate the same velocity of fiber shortening when ejecting against the same afterload. Finally, it requires that absolute values of velocity of fiber shortening can be reproducibly generated.

Some of these assumptions are of uncertain validity. The most important one, that of linearity and parallel shifts with changes in contractile state, is particularly doubtful. The force-velocity relation on which it is based is itself nonlinear, with a steep ascending limb at decreasing afterload. It is likely that the derived end-systolic wall stress–velocity of fiber shortening relation should follow the same behavior. In addition, the assumption of sensitivity to changes in contractile state has not been critically tested. In the initial study (12), only seven patients were studied in different contractile states. They were given dobutamine to increase contractile state and showed a modest increase in velocity of fiber shortening above the normal line. No patients received agents to decrease contractile state.

The present study was undertaken to address these two important assumptions. We determined whether the end-systolic wall stress–velocity of fiber shortening relation is indeed sensitive to changes in contractile state and whether it is linear and associated with parallel shifts in response to changes in contractile state over a physiologic range of afterload.

Methods

Surgical preparation. Eight piglets were studied at 4 to 6 weeks of age, using a study protocol approved by the Animal Research Committee of the University of California, San Francisco, and conforming with the "Position of the American Heart Association on Research Animal Use." After premedication with injection of ketamine hydrochloride (20 $mg \cdot kg^{-1}$ intramuscularly) and xylazine (2 $mg \cdot kg^{-1}$ intramuscularly), anesthesia was induced and maintained by chloralose infusion (100 $mg \cdot kg^{-1}$ intravenously every 2 h as needed). The piglet was intubated and ventilated with oxygen and air using a volume-regulated ventilator. Ventilation was adjusted to maintain arterial partial pressure of oxygen and carbon dioxide in the normal range throughout the study.

By means of a percutaneous approach, a 7F self-sealing sheath was placed in a femoral artery through which a balloon occlusion catheter was positioned in the mid-thoracic aorta. The balloon occlusion catheter was used to partially occlude the descending aorta and thereby increase afterload. A 5F self-sealing sheath was inserted in the axillary artery through a small incision in the right axilla, and a 5F micromanometric catheter (Millar Instruments) was advanced to the ascending aorta under fluoroscopic guidance.

Experimental protocol. To obtain the wall stress–velocity of fiber shortening relation, aortic pressure was acquired to videotape simultaneously with two-dimensionally directed M-mode echocardiography (ATL Ultramark 8 imaging system, Advanced Technology Laboratories) in each piglet in

JACC Vol. 23, No. 2
February 1994:514–24

six different conditions: in three contractile states (*baseline* and *increased* contractility during dobutamine infusion and *decreased* contractility after propranolol injection), each at two afterload states (normal and increased load by partial aortic occlusion).

Each piglet was first studied when the hemodynamic variables monitored (heart rate and arterial blood pressure) were stable for ≥15 min after the last adjustment in ventilation. This represents a baseline contractile state under normal load. Thereafter, the balloon in the descending aorta was partially inflated with saline solution to increase peak systolic pressure in the ascending aorta by ≥20 mm Hg and maintained for ≥15 s of hemodynamic stability. Data were obtained while ventilation was suspended, and the balloon was deflated after data acquisition. To increase contractile state, dobutamine was then infused at 10 $\mu g \cdot kg^{-1} \cdot min^{-1}$. After 15 min of hemodynamic stability, data were obtained at normal and increased afterload. The dobutamine infusion was stopped and after return to baseline hemodynamic status for 15 min, a baseline study was repeated. Finally, propranolol (1 $mg \cdot kg^{-1}$) was injected intravenously and the study repeated at normal and increased afterloads. To randomize data collection as much as possible, the acquisition of data during normal and increased afterload states within each contractile state was randomly varied. We found that the initial and repeat baseline measurements were not different, so that the data used for the baseline contractile state were from the initial measurements. Propranolol data were always obtained last because of its prolonged effects.

Data analysis. The end-systolic *meridional* wall stress (σ_m) and the rate-corrected mean velocity of fiber shortening were calculated from the minor-axis M-mode and aortic pressure data acquired on the same videotape applying standard technique (12,14,17). The end-systolic *circumferential* wall stress (σ_c) was calculated from the long- and short-axis dimensions measured from two-dimensional echocardiographic images obtained simultaneously with the M-mode echocardiogram. End-systolic pressure was determined as the point in time of the dicrotic notch in the aortic pressure tracing. We used this point because it is the closest approximation that can be obtained from noninvasive studies of carotid pulse tracings and, as such, is the point in the cardiac cycle currently used to derive the mean velocity of fiber shortening corrected for heart rate index. However, end-systole, defined as the point of maximal cross-bridge formation, is better approximated by the point in the cardiac cycle of maximal ventricular elastance. This point requires continuous measurement of ventricular pressure and volume, which is not feasible noninvasively. Moreover, it is not entirely clear that end-systolic stress is the most logical stress against which mean velocity of shortening tracks. It is quite possible that mean systolic stress or stress at peak pressure may be more appropriate. However, for the sake of this study, which attempts to validate an existing index of contractility, we believe that it is important to use the same timing points as those currently used.

Data were analyzed over five cardiac cycles and the mean values used for the subsequent calculations. Mean velocity of fiber shortening (Vcf) was calculated from the equation:

$$Vcf = \frac{D_{ed} - D_{es}}{D_{ed} \cdot ET}, \quad [1]$$

where D_{ed} is the left ventricular internal dimension at end-diastole (in cm), D_{es} is the left ventricular short-axis dimension at end-systole (in cm) and ET is the ejection time (in seconds).

Velocity of fiber shortening corrected for heart rate was calculated from the mean velocity of fiber shortening by dividing ejection time by the square root of the RR interval.

Left ventricular end-systolic meridional wall stress was calculated using the formula (18):

$$\sigma_m = \frac{1.35 \cdot P_{es} \cdot D_{es}}{4h_{es} \cdot \left(1 + \frac{h_{es}}{D_{es}}\right)}. \quad [2]$$

The calculation of meridional wall stress assumes that the relation between the short- and long-axes of the left ventricle remains constant. However, because of significant changes in loading and contractile states in our study, the relation between short- and long-axes may not remain constant. Consequently, circumferential wall stress, which is calculated from both short- and long-axis dimensions, was also measured in this study and plotted against velocity of fiber shortening in a fashion similar to meridional wall stress. Left ventricular end-systolic circumferential wall stress was calculated from a thick-walled ellipsoid model using the following formula (19):

$$\sigma_c = \frac{P_{es} \cdot D_{es} \cdot (2L_{es}^2 - D_{es}^2)}{4h_{es}\,(L_{es}^2 + D_{es} \cdot h_{es})}, \quad [3]$$

where σ_m is left ventricular end-systolic meridional wall stress (in $g \cdot cm^{-2}$), σ_c is left ventricular end-systolic circumferential wall stress (in $g \cdot cm^{-2}$), P_{es} is the aortic (and thus left ventricular) end-systolic pressure (in mm Hg), L_{es} is the left ventricular long-axis dimension at end-systole (in cm), h_{es} is the thickness of the posterior wall of the left ventricle (in cm), 1.35 is a conversion factor (which converts mm Hg to $g \cdot cm^{-2}$) and 4 is a constant that results from conversion of radius to internal dimension.

Statistical analysis. Statistical analyses were performed using effects coding and multiple linear regression analyses with dummy variables (19–21). To determine the sensitivity of the velocity of fiber shortening corrected for heart rate to changes in contractile state, we performed three different analyses. First, we performed two multiple regression analyses defining velocity of fiber shortening corrected for heart rate as the dependent variable, coded the presence of dobutamine or propranolol using two dummy drug variables (D1 and D2) and coded the interpiglet variability using seven dummy variables (P1 through P7) to represent the eight piglets (19–21). To incorporate afterload into the velocity of

fiber shortening corrected for heart rate (12), we first added afterload as a continuous variable σ and generated the following equation:

$$Vcf_c = b_0 + \sigma + \sum_{i=1}^{2} b_{Di}Di + \sum_{i=1}^{7} b_{Pi}Pi, \quad [4]$$

where σ represents either meridional or circumferential wall stress, b_0 represents the intercept of the equation and the other b's represent the coefficient for their respective variables.

In addition to using σ as a continuous variable for afterload, we created a second multiple linear regression model in which afterload was represented as the dummy variable A, assigning a data set during aortic occlusion a value of 1 and one during normal afterload without occlusion a value of −1. Thus, the equation was:

$$Vcf_c = b_0 + b_A A + \sum_{i=1}^{2} b_{Di}Di + \sum_{i=1}^{7} b_{Pi}Pi. \quad [5]$$

Using these two equations, b_0 represents the mean velocity of fiber shortening corrected for heart rate at zero load (that is, maximal velocity of fiber shortening corrected for heart rate) in equation 4, whereas b_0 represents the mean measured velocity of fiber shortening corrected for heart rate in equation 5.

Lastly, the afterload during the different contractile states without aortic occlusion was very different, with that during dobutamine infusion being the lowest and that during propranolol the highest. To remove the potential problem of nonoverlapping data, we performed a third analysis. We normalized wall stress across the different contractile states (in the absence of aortic occlusion) to the wall stress at baseline contractile state. We used a linear extrapolation of the high and normal afterload data from the dobutamine and propranolol states to derive the velocity of fiber shortening corrected for heart rate at baseline wall stress. We could not use a hyperbolic fit because we had only two data points for each contractile state. These derived values of velocity of fiber shortening corrected for heart rate are henceforth referred to as matched velocity of fiber shortening corrected for heart rate (Vcf_c/M). Now that velocity of fiber shortening corrected for heart rate is matched to baseline afterload, we did not need to incorporate an afterload term in the multiple regression analysis and thus derived the third equation to test contractile sensitivity as:

$$Vcf_c/M = b_0 + \sum_{i=1}^{2} b_{Di}Di + \sum_{i=1}^{7} b_{Pi}Pi. \quad [6]$$

To determine whether the wall stress-velocity of fiber shortening relation is linear and shifts in a parallel fashion at different contractile states, we constructed a slope $S_{Vcf_c-\sigma}$ from both meridional and circumferential wall stress data obtained at each contractile state as:

$$S_{Vcf_c-\sigma} = \frac{[Vcf_c(A^0) - Vcf_c(A^+)] \cdot 1{,}000}{[\sigma(A^0) - \sigma(A^+)]}, \quad [7]$$

where A^0 represents normal afterload data and A^+ represents the afterload data at the same contractile state but during partial aortic occlusion. From these slopes in each piglet in each contractile state, we generated the regression equation:

$$S_{Vcf_c-\sigma} = b_0 + \sum_{i=1}^{2} b_{Di}Di + \sum_{i=1}^{7} b_{Pi}Pi. \quad [8]$$

To determine the statistical significance of any variable or set of variables, an F test was performed by dividing the mean square of that variable or set by the mean square of the residual error. The mean square of a set of variables was calculated by summing the sum of squares of the individual dummy variables and dividing it by the number of variables, because the mean square of a dummy variable is equal to its sum of squares (degrees of freedom for a variable in a linear regression model is 1). Results of multiple regression analysis are presented as mean value ± SEM. A p value ≤ 0.05 was considered statistically significant. All other data are presented as mean value ± SD.

Results

The raw data from all the piglets are presented in Table 1.

Is the velocity of fiber shortening corrected for heart rate sensitive to changes in contractile state? Applying the regression analysis using equation 4 and considering *meridional* wall stress as a continuous variable, the predicted overall velocity of fiber shortening corrected for heart rate at zero load was 1.66 circumferences/second (circ·s^{-1}) (Table 2). Dobutamine increased it significantly to 2.08 ± 0.07 circ·s^{-1}, whereas propranolol decreased it significantly to 1.35 ± 0.07 circ·s^{-1}. When *circumferential* wall stress was used as a continuous variable, the results were similar (Table 3). The regression analysis applying equation 5 (afterload coded as a discontinuous variable, depending on whether or not the descending aorta was partially occluded) showed that the overall mean velocity of fiber shortening corrected for heart rate was 1.30 circ·s^{-1}, increasing significantly with dobutamine to 1.91 ± 0.05 circ·s^{-1} and decreasing significantly with propranolol to 0.78 ± 0.05 circ·s^{-1} (Table 4).

When we instead matched the velocity of fiber shortening (Vcf_c/M) during dobutamine and propranolol administration to baseline wall stress and then performed the regression analysis (equation 6), we again found that the effects of changes in contractile state were significant (Table 5), with dobutamine predicted to increase matched velocity of fiber shortening corrected for heart rate to 1.91 ± 0.09 circ·s^{-1} (140% of baseline) and propranolol predicted to decrease it to 1.05 ± 0.09 circ·s^{-1} (to 77% of baseline).

Thus, by all three regression analyses and using either meridional or circumferential wall stress, velocity of fiber

Table 1. Data From Individual Piglets During Baseline and Increased and Decreased Contractile States

Piglet No.	State	P_{es} (mm Hg)	D_{ed} (cm)	D_{es} (cm)	L_{es} (cm)	h_{es} (cm)	ET_c (s)	Vcf_c (circ·s^{-1})	σ_m (g·cm^{-2})	σ_c (g·cm^{-2})	Slope/σ_m	Slope/σ_c
1	B	63	1.59	0.97	3.3	0.77	0.250	1.55	15	35.5	−14.18	−9.65
	B+A	100	2.28	1.77	3.8	0.63	0.286	0.77	70	116.26	. . .	. . .
	D	46	1.40	0.73	2.7	0.97	0.218	2.2	5.01	15.2	−36.41	−23.72
	D+A	60	2.04	1.25	2.8	0.59	0.294	1.32	29.18	52.31	. . .	. . .
	P	70	2.45	1.73	3.5	0.53	0.313	0.93	59	93.3	. . .	. . .
	P+A										. . .	. . .
2	B	65	1.30	0.45	2.5	1.16	0.361	1.81	2.4	11.45	−13.95	−5.24
	B+A	98	1.88	0.68	3.0	0.89	0.377	1.69	11	34.18	. . .	. . .
	D	56	1.5	0.82	2.0	0.96	0.210	2.14	7.4	18.3	−54.12	−34.07
	D+A	93	1.62	1.00	1.9	0.99	0.207	1.68	15.9	31.76	. . .	. . .
	P	60	1.97	1.25	2.8	1.09	0.423	0.87	12.4	26.4	−7.38	−3.37
	P+A	75	2.38	1.62	3.4	0.9	0.408	0.78	29.2	53.1	. . .	. . .
3	B	50	1.47	0.92	2.4	1.08	0.302	1.24	6.2	16.83	−35.88	−20.1
	B+A	64	1.62	1.22	2.6	0.76	0.323	0.77	21.3	40.2	. . .	. . .
	D	42	1.50	1.00	2.2	0.82	0.204	1.65	9.5	19.64	−53.05	−36.71
	D+A	65	1.55	1.26	2.3	0.69	0.231	0.81	25.9	43.32	. . .	. . .
	P	32	1.70	1.70	3.1	0.68	0.319	0.84	19.3	30.34	−8.18	−4.71
	P+A	94	1.74	1.74	3.5	0.74	0.353	0.57	52.3	87.64	. . .	. . .
4	B	90	1.53	0.88	3.4	1.04	0.274	1.55	11.8	34.1	−21.43	−8.82
	B+A	108	1.73	0.97	3.7	1.06	0.300	1.46	15.6	44.3	. . .	. . .
	D	109	1.32	0.51	2.5	1.19	0.241	2.55	4.75	20.85	−69.64	−21.55
	D+A	138	1.60	0.59	2.8	1.13	0.275	2.3	8.34	32.47	. . .	. . .
	P	100	2.52	1.66	4.0	0.72	0.348	0.98	54.3	98	−14.59	−4.92
	P+A	139	3.02	2.24	4.4	0.81	0.364	0.71	95.3	152.9	. . .	. . .
5	B	137	2.90	2.09	3.6	0.72	0.309	0.97	98.8	148.13	−3.06	−5.14
	B+A	156	2.93	1.96	3.6	0.71	0.375	0.88	108.6	165.63	. . .	. . .
	D	143	2.85	1.45	2.5	1.02	0.200	2.3	40.3	68.37	−4.73	−8.14
	D+A	168	2.98	1.55	2.7	1.04	0.190	2.16	50.6	85.63	. . .	. . .
	P	147	3.26	2.53	3.8	0.67	0.313	0.7	145.5	193.33	−1.03	−2.68
	P+A	166	3.29	2.55	4.0	0.68	0.359	0.63	164.3	223.05	. . .	. . .
6	B	90	0.67	1.86	3.4	1.15	0.356	1.78	6.48	24.1	−53.11	−17.94
	B+A	118	1.14	2.23	3.8	1.17	0.370	1.31	19.1	50.3	. . .	. . .
	D	105	0.37	1.28	2.8	1.37	0.286	2.5	2.1	13.2	−114.29	−24.39
	D+A	127	0.44	1.35	3.2	1.23	0.288	2.3	4.0	21.37	. . .	. . .
	P	98	1.33	2.20	3.7	0.81	0.351	1.13	33.8	69.77	−7.16	−10.3
	P+A	115	1.55	2.25	4.0	0.82	0.350	0.89	47.94	93.13	. . .	. . .
7	B	78	3.39	2.23	3.6	0.93	0.344	1.0	44.56	65.15	−6.56	−2.7
	B+A	95	3.46	2.31	3.9	0.91	0.355	0.94	58.4	87.4	. . .	. . .
	D	70	2.46	1.39	2.2	1.02	0.254	1.71	18.6	29.5	−14.09	−18.6
	D+A	86	3.12	1.96	2.8	1.2	0.246	1.5	35.1	40.79	. . .	. . .
	P	72	3.44	2.67	3.6	0.85	0.286	0.78	57.9	69.76	−4.76	−5.2
	P+A	90	3.08	2.44	3.7	0.84	0.269	0.77	60	88.9	. . .	. . .
8	B	130	3.38	1.95	3.2	0.75	0.400	1.06	82.5	120.4	−5.67	−4.7
	B+A	155	3.57	2.45	3.4	0.72	0.410	0.76	135.4	168.7	. . .	. . .
	D	127	2.91	1.51	2.6	0.92	0.258	1.86	43.97	71.88	−15.91	−14.88
	D+A	156	3.22	1.9	2.9	0.99	0.277	1.5	66.6	96.08	. . .	. . .
	P	116	3.58	2.78	3.8	0.69	0.328	0.68	126.4	151.1	−1.71	−1.3
	P+A	132	3.76	3.05	4.2	0.67	0.304	0.62	166.3	198.2	. . .	. . .

A = increased afterload state; B = baseline contractile state; D = dobutamine infusion; D_{ed} = end-diastolic short-axis dimension; D_{es} = end-systolic short-axis dimension; ET_c = heart rate–corrected ejection time; h_{es} = end-systolic wall thickness; L_{es} = end-systolic long-axis manual dimension; P = propranolol bolus injection; P_{es} = end-systolic pressure; σ_c = end-systolic circumferential wall stress; σ_m = end-systolic meridional wall stress; Slope/σ_c = slope of the relation between end-systolic circumferential wall stress and heart rate–corrected velocity of fiber shortening; Slope/σ_m = slope of the relation between end-systolic meridional wall stress and heart rate–corrected velocity of fiber shortening; Vcf_c = heart rate–corrected velocity of fiber shortening.

Table 2. Multiple Linear Regression of Velocity of Fiber Shortening Corrected for Heart Rate as the Dependent Variable, Considering Meridional Wall Stress (σ_m) as a Continuous Variable (equation 4)

			Drug Variable		Interanimal Variability						
Variable	b_0	σ_m	D1	D2	P1	P2	P3	P4	P5	P6	P7
b	1.66	−0.01	0.42	−0.31	−0.08	−0.07	−0.51	0.22	0.31	0.11	−0.20
SEM		0.002	0.07	0.07	0.10	0.11	0.10	0.10	0.12	0.11	0.10
F test		18.98	40.60	19.58				5.94			
p value		0.001*	<0.001*	<0.001*				Coefficients combined <0.05*			

*The coefficient of the variable or set of variables is statistically significant. All values are in circumferences/second (circ·s^{-1}), except for σ_m, which is in g·cm^{-2}. The set of drug variables (D1, D2) codes dobutamine data as (1, 0), propranolol data as (0, 1) and control data as (−1, −1). The set of variables for interanimal variability (P1 through P7, representing the eight piglets) is similarly coded by effects. The regression equation was statistically significant (r = 0.93, p = 0.0001). b_0 = the intercept of the equation, or overall mean velocity of fiber shortening corrected for heart rate.

Table 3. Multiple Linear Regression of Velocity of Fiber Shortening Corrected for Heart Rate as the Dependent Variable, Considering Circumferential Wall Stress (σ_c) as a Continuous Variable (equation 4)

			Drug Variable		Interanimal Variability						
Variable	b_0	σ_m	D1	D2	P1	P2	P3	P4	P5	P6	P7
b	1.81	−0.01	0.37	−0.27	−0.07	−0.13	−0.57	0.27	0.45	0.14	−0.28
SEM		0.001	0.06	0.07	0.09	0.11	0.1	0.09	0.13	0.1	0.09
F test		26.38	34.71	16.71				9.81			
p value		0.001*	<0.001*	<0.001*				Coefficients combined <0.05*			

*The coefficient of the variable or set of variables is statistically significant. All values are in circumferences/second (circ·s^{-1}), except for σ_c, which is in g·cm^{-2}. See Table 1 for definition of other variables. The regression equation was statistically significant (r = 0.94, p = 0.0001).

Table 4. Multiple Linear Regression of Velocity of Fiber Shortening Corrected for Heart Rate as the Dependent Variable, Considering Wall Stress as a Dummy Variable (equation 5)

		Afterload Variable	Drug Variable		Interanimal Variability						
Variable	b_0	A	D1	D2	P1	P2	P3	P4	P5	P6	P7
b	1.3	−0.15	0.61	−0.52	−0.08	0.2	−0.32	0.29	−0.04	0.35	−0.18
SEM		0.04	0.05	0.05	0.11	0.10	0.10	0.10	0.10	0.10	0.10
F test		15.74	134.14	96.34				5.85			
p value		<0.001*	<0.001*	<0.001*				Coefficients combined <0.05*			

*The coefficient of the variable or set of variables is statistically significant. Afterload variable (A) is coded as 1 for high afterload (aortic occlusion) and −1 for normal afterload (control). See Table 2 for definition of the other variables. The regression equation was statistically significant (r = 0.92, p = 0.0001).

Table 5. Multiple Linear Regression of Velocity of Fiber Shortening Corrected for Heart Rate Matched to Control Preload (equation 6) as the Dependent Variable

		Drug Variable		Interanimal Variability						
Variable	b_0	D1	D2	P1	P2	P3	P4	P5	P6	P7
b	1.44	0.47	−0.39	0.001	0.39	−0.09	0.50	−0.24	0.23	−0.37
SEM		0.09	0.09	0.16	0.16	0.16	0.16	0.16	0.16	0.16
F test		29.7	20.8				3.5			
p value		<0.001*	<0.001*				Coefficients combined >0.05*			

*The coefficient of the variable or set of variables is statistically significant. See Table 2 for definition of the variables. The regression equation was statistically significant (r = 0.90, p = 0.001).

Table 6. Multiple Linear Regression of the Slope of Velocity of Fiber Shortening–Meridional Wall Stress Relation at Each Contractile State (equation 8) as the Dependent Variable

		Drug Variable		Interanimal Variability						
Variable	b_0	D1	D2	P1	P2	P3	P4	P5	P6	P7
b	−24.23	−24.03	19.03	8.45	−8.87	−8.14	−10.99	21.29	−33.96	15.76
SEM		5.69	5.98	12.81	10.52	10.52	10.52	10.52	10.52	10.52
F test		17.83	10.14				2.8			
p value		0.001*	0.007*				Coefficients combined >0.05*			

*The coefficient of the variable or set of variables is statistically significant. All variables are in circ·s^{-1}·g^{-1}·cm^2. See Table 1 for definition of the variables. The regression equation was statistically significant (r = 0.86, p = 0.01). Circ·s = circumferences per second.

shortening corrected for heart rate is very sensitive to changes in contractile state.

Does the wall stress-velocity of fiber shortening relation shift in a parallel fashion? Assuming a linear relation between wall stress and velocity of fiber shortening, the two loading conditions during each contractile state allowed us to construct slopes of the wall stress-velocity of fiber shortening relation for each contractile state and compare these slopes. If the relation indeed shifts in a parallel fashion, these slopes should be the same. However, by multiple regression analysis (equation 8, Table 6), we found that the slope obtained during dobutamine infusion was significantly steeper (−48.26 ± 5.69 circ·s^{-1}·g^{-1}·cm^2) and that during propranolol was significantly less steep (−5.2 ± 5.98 circ·s^{-1}·g^{-1}·cm^2) than the mean overall slope (−24.23 circ·s^{-1}·g^{-1}·cm^2) when meridional wall stress was used to construct these slopes. When circumferential wall stress was used to construct these slopes, they behaved in a similar fashion (Table 7): Dobutamine produced significantly steeper slopes (−22.76 ± 1.57 circ·s^{-1}·g^{-1}·cm^2) and propranolol produced less steep slopes (−4.07 ± 1.65 circ·s^{-1}·g^{-1}·cm^2) than the mean overall slope (−12.04 circ·s^{-1}·g^{-1}·cm^2). A typical example of the slopes derived from an individual piglet is presented in Figure 2.

Such changes in the steepness of these slopes observed at varying contractile states leads to the question of linearity of this relation.

Is the wall stress–velocity of fiber shortening relation linear? Because dobutamine reduced end-systolic dimensions and produced vasodilation and relative thickening of the left ventricular wall, the measured mean meridional wall stress obtained during dobutamine infusion was lower (15.75 ± 14.73 g·cm^{-2}), whereas that after propranolol was higher (60.04 ± 42.72 g·cm^{-2}) than at baseline (33.19 ± 38.07 g·cm^{-2}). Thus, the steeper slopes seen during dobutamine infusion most likely represent the rapidly ascending limb of a rectangular hyperbola, whereas the less steeper slope obtained after a propranolol bolus injection may represent the plateau phase (Fig. 3).

Discussion

Sensitivity of the index to changes in contractility. We found that velocity of fiber shortening corrected for heart rate is a sensitive index of myocardial contractility when corrected for afterload. However, the assumptions that the wall stress–velocity of fiber shortening relation is linear and shifts in a parallel manner in response to changes in contractility are not valid over a physiologic range of afterloads. Rather, from our data and the muscle property on which it is based, we speculate that the wall stress–velocity of fiber shortening relation approximates a rectangular hyperbola similar to that of the force-velocity relation from which it is derived. Thus, the current use of end-systolic wall stress–velocity of fiber shortening corrected for heart rate as a single-beat index of contractility is inappropriate.

The sensitivity of velocity of fiber shortening corrected for heart rate as an index of myocardial contractility is clearly demonstrated from our data, whether we 1) incorporated afterload using a continuous variable for wall stress or as a dummy variable coded for the presence or absence of increased afterload, 2) we used meridional or circumferential wall stress, or 3) matched velocity of fiber shortening corrected for heart rate from the altered contractile states to

Table 7. Multiple Linear Regression of the Slope of Velocity of Fiber Shortening–Circumferential Wall Stress Relation at Each Contractile State (equation 8) as the Dependent Variable

		Drug Variable		Interanimal Variability						
Variable	b_0	D1	D2	P1	P2	P3	P4	P5	P6	P7
b	−12.04	−10.72	7.97	−0.66	−2.19	−8.47	0.27	6.72	−5.51	4.76
SEM		1.57	1.65	3.53	2.9	2.9	2.9	2.9	2.9	2.9
F test		46.65	23.37				2.97			
p value		0.001*	<0.001*				Coefficients combined >0.05*			

*The coefficient of the variable or set of variables is statistically significant. All variables are in circ·s^{-1}·g^{-1}·cm^2. See Table 1 for definition of the variables. The regression equation was statistically significant (r = 0.92, p < 0.001). Circ·s = circumferences per second.

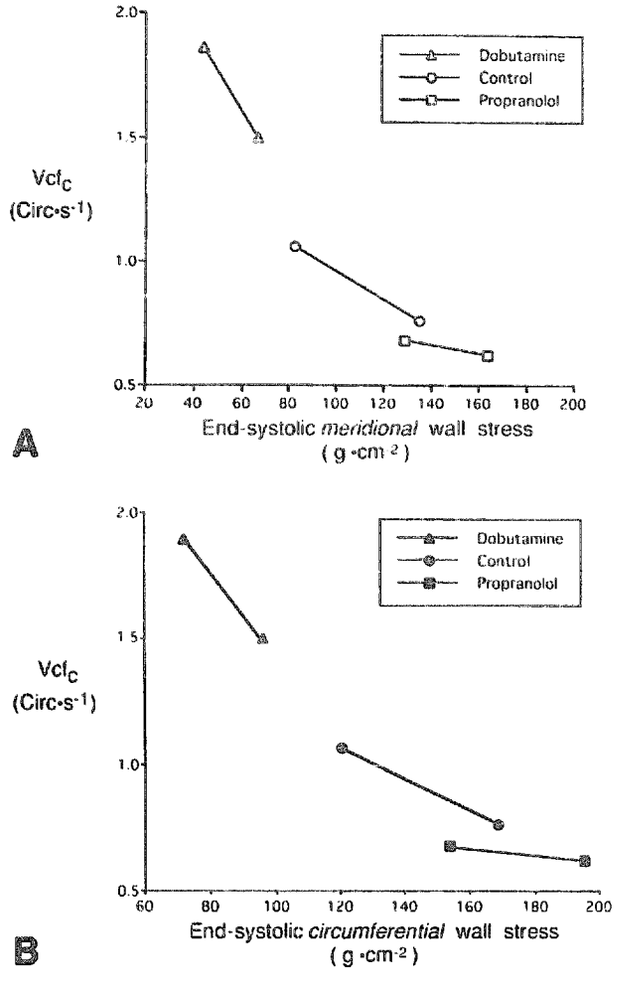

Figure 2. Representative data from one piglet, showing lines drawn between data obtained by calculating both meridional (A) and circumferential (B) wall stress at normal and increased load during control, increased (dobutamine) and decreased (propranolol) contractile states. Circ·s^{-1} = circumferences per second, Vcf_c = mean velocity of fiber shortening corrected for heart rate.

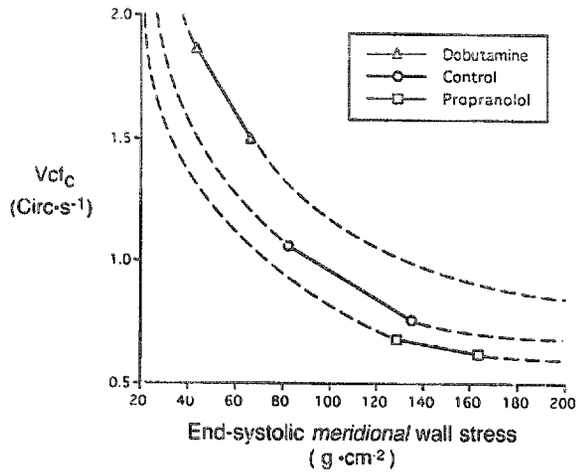

Figure 3. Suggested hyperbolic fit of the end-systolic wall stress–velocity of fiber shortening relation at different contractile states from those depicted by data from Figure 2A. Abbreviations as in Figure 2.

baseline wall stress. Colan et al. (12) infused dobutamine at a dose of 5 $\mu g \cdot kg^{-1} \cdot min^{-1}$ to increase contractility in seven subjects and observed increased values at all levels of wall stress. We found that infusion of a larger dose of dobutamine caused an even greater increase in velocity of fiber shortening corrected for heart rate in piglets and demonstrated that propranolol decreased it to a large extent.

Use as single-beat index of contractility. Although velocity of fiber shortening corrected for heart rate is sensitive to changes in myocardial contractility, attempts to use it as a single-beat index of contractility (13–16) are based on invalid assumptions and should be discouraged. Attempts to assess ventricular function in terms of other single-beat indexes have uniformly been ill-fated. For example, the maximal first derivative of left ventricular pressure (dP/dt_{max}) was initially a very popular single-beat index (22) until it was found to be significantly heart rate and preload dependent (23). Moreover, the use of dP/dt_{max} as an index of myocardial contractility depends on its being an isovolumetric event, whereas other studies (24) have shown that this is not always the case, demonstrating that dP/dt_{max} depends on afterload as well. Maximal velocity of shortening (V_{max}) was also introduced as a sensitive index of myocardial contractility that was independent of preload, leading to its use as a single-beat index of myocardial contractility in numerous studies (8,9,25). However, subsequent work (26–29) has shown that V_{max} is length dependent and difficult to extrapolate, thereby leading to its disuse. Ejection fraction is a useful screening measurement of global systolic performance, but its significant load dependence invalidates its use as an accurate index of contractility (30,31). All other single-beat indexes to date have met a similar fate (32).

Similar to these other indexes, the wall stress–velocity of fiber shortening relation corrected for heart rate cannot be used as a single beat index of contractility. In addition to its failure to satisfy the assumptions of linearity and parallel shifts, it was associated with a large and significant interanimal variability. Thus, absolute data from normal hearts may lie in a set of data that includes hearts of abnormal contractile state and thus may not be a sensitive index. Although we found the index to be sensitive within an animal by generating both normal and abnormal data, the sensitivity between animals was not tested. Deriving absolute data in one state in one subject may not allow the investigator to be certain where that data point lies within that subject's range of function. This intersubject variability was not specifically evaluated in our study, but the wide range of normal values is disturbing.

Nonlinearity of the wall stress–velocity of fiber shortening relation. Most disturbing is the clear failure of the wall stress–velocity of fiber shortening relation to meet the assumptions of linearity and parallel shifts necessary to use individual velocity of fiber shortening corrected for heart

rate data to estimate contractile state. The curvilinearity of this relationship became apparent when it was noted that the relation did not shift in a parallel fashion with changes in contractile state, but rather became steeper as dobutamine increased contractile state (and concomitantly decreased wall stress) and flatter as propranolol decreased contractile state (and increased wall stress). Although dobutamine clearly increased the velocity of fiber shortening corrected for heart rate, thus demonstrating a sensitivity of the index to contractile state, current use dictates that it should have done so while maintaining the same slope of the relation. To clarify this argument, we present Figure 4, A to C. Figure 4A demonstrates the relation as currently used, with two hypothetical single-beat points that represent data that would currently be considered to be of increased (point 1) and normal (point 2) contractile states. Although this interpretation may be correct, it may not. It is also possible that point 1 represents a single beat from a heart of normal contractile state and decreased afterload (Fig. 4B). As afterload decreases into the range that we saw during dobutamine infusion, the hyperbolic curve of normal data starts to bend more steeply and thus passes through point 1. A typical example of this may be seen in a patient with infection, fever and anemia, all of which may decrease afterload and not necessarily increase contractile state. This is an alternative explanation of the results of a study that, using this index, evaluated patients early in the phase of HIV infection. The authors (16) concluded that these patients have hearts that are functioning at an increased contractile state. Alternatively, we propose that the data are compatible with the more likely situation that these patients, exposed to infection and often anemic, have a normal heart that is functioning at normal contractile states but in the presence of decreased afterload.

The same concept can be applied to point 2 in Figure 4C. In this figure, two points at high (●) and normal (Δ) afterloads depict a decreased contractile state. At low afterloads, however, the curve bends sharply to pass through point 2 (★). Therefore, point 2 could represent a depressed contractile state at low afterload, rather than a normal contractile state, as implied by the current use of the wall stress–velocity of fiber shortening relation. A typical example may be seen in a patient with dilated cardiomyopathy receiving afterload-reducing agents.

Therefore, the wall stress–velocity of fiber shortening relation may appear linear if only the flat portion of the hyperbolic curve is investigated. At low afterloads, the curvilinearity of this relation becomes more apparent. Previous studies (12) have not investigated the relation at low afterload, evaluating contractility only at normal and increased (during methoxamine infusion) afterload.

Load dependence of contractility. Lastly, the validity of the use of end-systolic wall stress–velocity of fiber shortening relation as a single-beat index of contractility assumes not only that the index is load independent but that contractility itself is load independent (12). However, it has become

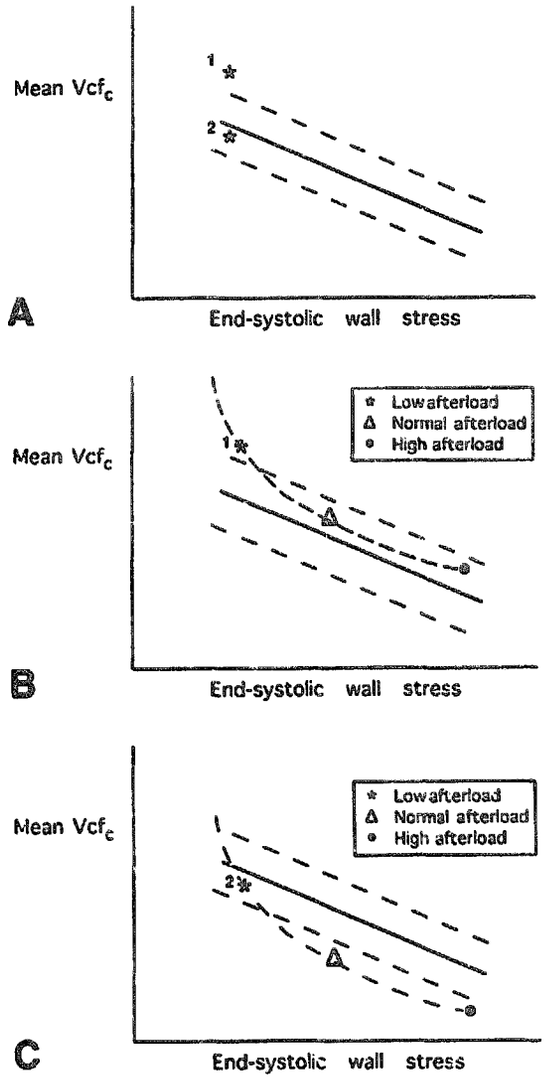

Figure 4. Hypothetical single-beat values of velocity of fiber shortening corrected for heart rate (Vcf_c) obtained from two subjects. **A**, Data point 1 lies above the 2 SD line of the relation, suggesting that the heart is functioning at an increased contractile state, whereas data point 2 lies within the 2 SD line, suggesting that the contractile state is normal. **B**, An alternative explanation of data point 1 is that the contractile state is normal, but afterload is decreased as demonstrated by the hypothetical hyperbolic relation (– – –). **C**, An alternative explanation of data point 2 is that contractile state is depressed, but the point may fall within the so-called normal range as the afterload is decreased.

increasingly evident that this is not the case. If contractility is defined in terms of the interplay between the myofilament and available calcium, then alterations in contractility are affected by any process that either increases available intracellular calcium during excitation of the myocyte or increases the sensitivity of myofilament to that calcium. Using this definition, the traditional concept that views contractility, preload and afterload as independent determinants of cardiac performance is invalid. Direct effects of preload on contractility have been shown in isolated cardiac muscle preparations (33–35) and the intact heart (36). These studies

suggest that initial muscle length influences myocardial contractility; following a stretch in the cardiac muscle, the process of activation of the contractile system is heightened. This is caused by both a larger increase in available intracellular calcium at greater initial lengths and an increased sensitivity of the myofilament to that calcium. Such length dependence of activation suggests that there is a constant interplay between myocardial fiber length (preload) and contractility and explains the Frank-Starling mechanism in terms of alterations in contractility, rather than as an independent phenomenon (35). Dependence of contractility on afterload has also been demonstrated in the intact circulation (37) and in the isolated heart (38). Contractility, as defined by both end-systolic (end-systolic pressure-volume relation) and early systolic (dP/dt_{max}–end-diastolic volume relation) indexes, increases in response to an increase in afterload independent of the indirect effects of beta-adrenergic stimulation. This finding is in part caused by shortening deactivation of the myofilament, although there is a constant interaction between forces that augment and those that depress contractile performance during ejection (39). Thus, the interaction between load and contractility is complex and pervasive throughout the cardiac cycle. The concept that one can evaluate changes in contractility independent from changes in preload and afterload is not valid; therefore, any index that does not consider the interplay must fall short as an index of contractility.

Conclusions. The velocity of fiber shortening corrected for heart rate is sensitive to changes in contractile state. As such, it may be very useful in the temporal noninvasive evaluation of individual patients undergoing drug or surgical interventions or in the definition of the natural history of a disease process. However, its current use as a single-beat index of contractility by comparing isolated data points in an individual subject with normal linear tolerance bands is very suspect for a variety of reasons. From this study, it appears that the wall stress–velocity of fiber shortening relation on which the index is based approximates a rectangular hyperbola rather than a straight line; thus, isolated single data points above the normal region may be achieved by decreased afterload, as well as by the currently accepted presumption of increased contractility. We believe that end-systolic wall stress–velocity of fiber shortening relation should not continue to be used as a single-beat index of contractility; instead we propose that it should be calculated over a range of load in each subject if repeated measures under different conditions are not made. It is possible to obtain such data noninvasively by short-term maneuvers that alter load, such as the use of tilt table testing. Moreover, an appreciation of the true nature of the intrinsic properties of the heart and the interdependence of load, contractility and heart rate should allow the clinical investigator to apply in a rational fashion a host of indexes of contractile function noninvasively.

References

1. Suga H, Sagawa K. Instantaneous pressure-volume relationship and their ratio in the excised supported canine left ventricle. Circ Res 1974;35: 117–26.
2. Glower DD, Spratt JA, Snow ND, et al. Linearity of the Frank-Starling relationship in the intact heart: the concept of preload recruitable stroke work. Circulation 1985;71:994–1009.
3. Anderson PA, Rankin JS, Arentzen CE, Anderson RW, Johnson EA. Evaluation of the force-frequency relationship as a descriptor of the inotropic state of canine left ventricular myocardium. Circ Res 1976;39: 832–9.
4. Anderson PA, Manring A, Johnson EA. The force-frequency relationship: a basis for a new index of cardiac contractility. Circ Res 1973;33: 665–71.
5. Cohn PF. Evaluation of inotropic contractile reserve in ischemic heart disease using post extrasystolic potentiation. Circulation 1980;61:1071–5.
6. Karliner JS, Gault JH, Eckberg DL. Mean velocity of fiber shortening: a simplified measure of left ventricular myocardial contractility. Circulation 1971;44:323–33.
7. Cooper RH, O'Rourke RA, Karliner JS. Comparison of ultrasound and cineangiographic measurements of the mean rate of circumferential fiber shortening in man. Circulation 1972;46:914–23.
8. Sonnenblick EH. Force velocity relations in mammalian heart muscle. Am J Physiol 1962;202:931–9.
9. Sonnenblick EH, Parmley WW, Urschel CW. Contractile state of the heart as expressed by force-velocity relations. Am J Cardiol 1969;23:488–503.
10. Hill AV. The heat of shortening and the dynamic constants of muscle. Proc Roy Soc Lond 1938;Series B, 126:136–95.
11. Hill AV. The abrupt transition from rest to activity in muscle. Proc Roy Soc Lond 1949;Series B, 136:399–420.
12. Colan SD, Borow KM, Neumann A. Left ventricular end-systolic wall stress-velocity of fiber shortening relation: a load-independent index of myocardial contractility. J Am Coll Cardiol 1984;4:715–24.
13. Colan SD, Eckardt T, Wernovsky G, Sholler GF, Sanders SP, Castenada AR. Myocardial performance after arterial switch operation for transposition of the great arteries with intact ventricular septum. Circulation 1988;78:132–41.
14. Colan SD, Sanders SP, Ingelfinger JR, Harmon W. Left ventricular mechanics and contractile state in children and young adults with end-stage renal disease: effect of dialysis and renal transplantation. J Am Coll Cardiol 1987;10:1085–94.
15. Graham TP Jr, Franklin RCG, Wyse RKH, Gooch V, Deanfield JE. Left ventricular wall stress and contractile function in childhood: normal and comparison of Fontan repair versus palliation only in patients with tricuspid atresia. Circulation 1986;74 Suppl I:I61–9.
16. Lipshultz SE, Chanock S, Sanders SP, Colan SD, Perez-Atayde A, McIntosh K. Cardiovascular manifestations of human immunodeficiency virus infection in infants and children. Am J Cardiol 1989;63:1489–97.
17. Rein AJ, Sanders SP, Colan SD, Parness IA, Epstein M. Left ventricular mechanics in the normal newborn. Circulation 1987;76:1029–36.
18. Grossman W, Jones D, McLaurin LP. Wall stress and patterns of hypertrophy in the human left ventricle. J Clin Invest 1975;56:56–64.
19. Falsetti HL, Mates RE, Grant C, Greene DG, Bunnell IL. Left ventricular wall stress calculated from one-plane cineangiography. Circ Res 1970;25:71–83.
20. Glantz SA, Slinker BK. Primer of Applied Regression and Analysis of Variance. New York: McGraw-Hill, 1990.
21. Slinker BK, Glantz SA. Missing data in two-way analysis of variance. Am J Physiol 1990;258:R291–7.
22. Teitel DF, Klautz R, Steendijk P, Van der Velde ET, Van Bel F, Baan J. The end-systolic pressure-volume relationship in the newborn lamb: effects of loading and inotropic interventions. Pediatr Res 1991;29: 473–82.
23. Gleason WL, Braunwald E. Studies on the first derivative of the ventricular pressure pulse in man. J Clin Invest 1962;41:80–6.
24. Mason DT. Usefulness and limitations of rate rise of intraventricular pressure (dP/dt) in the evaluation of myocardial contractility in man. Am J Cardiol 1969;23:516–27.

25. Van Den Bos GC, Elzinga G, Westerhof N, Noble MIM. Problems in the use of indices of myocardial contractility. Cardiovasc Res 1973;7:834–48.
26. Ross JJ, Covell JW, Sonnenblick EH, Braunwald E. Contractile state of the heart characterized by force-velocity relations in variably afterloaded and isovolumic beats. Circ Res 1966;18:149–63.
27. Pollack GH. Maximum velocity as an index of contractility in cardiac muscle: a critical evaluation. Circ Res 1970;26:111–27.
28. Parmley WW, Chuck H, Yeatman H. Comparative evaluation of the specificity and sensitivity of isometric indices of contractility. Am J Physiol 1975;228:506–10.
29. Quinones MA, Gaasch WH, Alexander JK. Influence of acute changes in preload, afterload, contractile state and heart rate on ejection and isovolumic indices of myocardial contractility in man. Circulation 1976; 53:293–302.
30. Robotham JL, Takata M, Berman M, Harasawa Y. Ejection fraction revisited. Anesthesiology 1991;74:172–83.
31. MacGregor DC, Covell JW, Mahler F. Relations between afterload, stroke volume and the descending limb of Starling's curve. Am J Physiol 1974;227:884–90.
32. Elzinga G, Westerhof N. How to quantify pump function of the heart. Circ Res 1979;44:303–8.
33. Allen DG, Kurihara S. The effects of muscle length on intracellular calcium transients in mammalian cardiac muscle. J Physiol 1982;327: 79–94.
34. Allen DG, Nichols CG, Smith GL. The effect of changes in muscle length during diastole on the calcium transient in ferret ventricular muscle. J Physiol 1988;406:359–70.
35. Lakatta EG, Jewell BR. Length-dependent activation: its effect on the length-tension relation in cat ventricular muscle. Circ Res 1977;40:251–7.
36. Tucci PJ, Bregagnollo EA, Spadaro J, Cicogna AC, Ribeiro MC. Length-dependence of activation studied in the isovolumic blood-perfused dog heart. Circ Res 1984;55:59–66.
37. van der Velde ET, Burkhoff D, Steendijk P, Karsdon J, Sagawa K, Baan J. Nonlinearity and load sensitivity of end-systolic pressure-volume relation of canine left ventricle in vivo. Circulation 1991;83:315–27.
38. Nishioka O, Maruyama Y, Ashikawa K, et al. Load dependency of end-systolic pressure-volume relations in isolated, ejecting canine hearts. Jpn Heart J 1988;29:709–22.
39. Hunter WC. End-systolic pressure as a balance between opposing effects of ejection. Circ Res 1989;64:265–75.